Journal of Applied Polymer Science

Poly(ε-caprolactone)-*Graft*-Poly(*N*-isopropylacrylamide) Amphiphilic Copolymers Prepared by a Combination of Ring-Opening Polymerization and Atom Transfer Radical Polymerization: Synthesis, Self-Assembly, and Thermoresponsive Property

Mingming Li, Guorong Shan, Yongzhong Bao, Pengju Pan
State Key Laboratory of Chemical Engineering, Department of Chemical and Biological Engineering, Zhejiang University, Hangzhou 310027, China
Correspondence to: P. Pan (E-mail: panpengju@zju.edu.cn)

ABSTRACT: Thermoresponsive graft copolymers of ε-caprolactone and *N*-isopropylacrylamide were synthesized by a combination of ring-opening polymerization and the sequential atom transfer radical polymerization (ATRP). The copolymer composition, chemical structure, and the self-assembled structure were characterized. The graft length and density of the copolymers were well controlled by varying the feed ratio of monomer to initiator and the fraction of chlorides along PCL backbone, which is acting as the macroinitiator for ATRP. In aqueous solution, PCL-*g*-PNIPAAm can assemble into the spherical micelles which comprise of the biodegradable hydrophobic PCL core and thermoresponsive hydrophilic PNIPAAm corona. The critical micelle concentrations of PCL-*g*-PNIPAAm were determined under the range of 6.4–23.4 mg/L, which increases with the PNIPAAm content increasing. The mean hydrodynamic diameters of PCL-*g*-PNIPAAm micelles depend strongly on the graft length and density of the PNIPAAm segment, allowing to tune the particle size within a wide range. Additionally, the PCL-*g*-PNIPAAm micelles exhibit thermosensitive properties and aggregate when the temperature is above the lower critical solution temperature. © 2014 Wiley Periodicals, Inc. J. Appl. Polym. Sci. **2014**, *131*, 41115.

KEYWORDS: biodegradable; micelles; stimuli-sensitive polymers

Received 10 February 2014; accepted 8 June 2014
DOI: 10.1002/app.41115

INTRODUCTION

The amphiphilic copolymers, having a large solubility difference between the hydrophilic and hydrophobic segments, are known to assemble into the nano-scaled polymeric micelles in an aqueous media. They have been drawn considerable academic interests because of the great potentials for biomedical applications.[1,2] These micelles usually have the unique core-shell structures, in which the hydrophobic moieties are segregated from the aqueous exterior to form an inner core surrounded by the hydrophilic segments. The hydrophobic core can encapsulate/solubilize the hydrophobic drugs, while the hydrophilic shell can stabilize the whole system. Considering the safety and biocompatibility, the biodegradable polyesters, for example, poly(ε-caprolactone) (PCL), poly(lactic acid) (PLA), and poly(lactide-*co*-glycolide) (PLGA) have been widely used as the hydrophobic segments of the amphiphilic copolymers.[3]

Recently, the stimuli-responsive amphiphilic copolymers and their self-assemblies have been received great attention because of their unique properties. Poly(*N*-isopropylacrylamide) (PNIPAAm) is one of the typical thermoresponsive polymers, exhibiting a lower critical solution temperature (LCST) at ~33°C.[4,5] PNIPAAm is hydrophilic at a temperature below LCST but hydrophobic above LCST. The biodegradable polyesters such as PCL and PLA have been copolymerized with PNIPAAm to prepare the stimulus responsive copolymers with the diverse macromolecular topologies, such as the diblock,[6–11] triblock,[12–15] star-shaped copolymers,[16–18] and the graft copolymers with the biodegradable polyesters as grafting chains.[19,20] These linear and star-shaped block copolymers can be synthesized by combining the ring-opening polymerization (ROP) of lactone monomer and living radical polymerization of NIPAAm, in which chain-end functionalization of the first block was necessary for initiating the living radical polymerization of the second block. In aqueous solution, the amphiphilic copolymers of biodegradable polyester and PNIPAAm can assemble into the thermoresponsive micelles comprised of the biodegradable cores. These micelles have been reported to exhibit thermosensitive release

Additional Supporting Information may be found in the online version of this article.

behavior for the hydrophobic drugs and can be eliminated from the body by hydrolytic or enzymatic degradation after its desired period of circulation. For example, Li and coworkers have prepared the PNIPAAm-*b*-PCL-*b*-PNIPAAm triblock copolymers by a combination of ROP and atom transfer radical polymerization (ATRP). In aqueous solution, these copolymers self-assemble into the spherical particles with a diameter ranging from 93 to 125 nm.[12] Zhang and coworkers have synthesized the PCL-*b*-PNIPAAm-*b*-PCL triblock copolymers by the sequential ROP and reversible addition-fragmentation chain transfer (RAFT) polymerization. The release behavior of drug-loaded PCL-*b*-PNIPAAm-*b*-PCL micelles is thermosensitive. When the temperature was increased to above LCST, the burst release of encapsulated drug was observed.[13]

For the biodegradable polymers in biomedical applications, the structural homogeneity is of critical importance to ensure that the structures and properties of degradation products change little during their service lives.[21] As compared to the biodegradable polyester/PNIPAAm block copolymers or graft copolymers bearing the biodegradable grafting chains, the graft copolymers comprising biodegradable backbones and pendent side chains have better structural homogeneity, because the degradation of such materials yields polymer fragments with relatively similar properties.[21] Although the thermoresponsive graft copolymers containing biodegradable polyester side chains have been studied,[19,20] few works have been reported on the synthesis and self-assembly studies of the thermoresponsive amphiphilic graft copolymers bearing the biodegradable polyester backbones.

As the common biodegradable polyesters do not contain pendent functional groups, the functionalization of its backbone is necessary to prepare the graft copolymers. Recently, several researchers have reported the pendent functionalization of PCL by halogenation.[22–29] The halogen-functionalized PCL can be conveniently prepared through the ring-opening copolymerization of caprolactone and halogen-substituted caprolactone. It has been reported that the halogen-substituted PCL can initiate the ATRP of vinyl monomers, allowing to prepare the graft copolymers by the "grafting from" strategy.[30] Moreover, the pendent halogens in biodegradable polyesters can be easily converted to azides, providing a straightforward "grafting onto" method to prepare the graft copolymers by azide/alkyne click chemistry.[31–36]

In this contribution, we first prepared the chloro-substituted PCL by ROP of unsubstituted and halogen-substituted caprolactones. A series of PCL-*g*-PNIPAAm amphiphilic graft copolymers were then synthesized by the atom transfer radical polymerization with activators regenerated by electron transfer (ARGET ATRP) using the chloro-substituted PCL as macroinitiator. The graft length and density of PCL-*g*-PNIPAAm were controlled by varying the feed ratio of monomer to initiator and the content of chloro functionality along PCL backbone. The chemical structures of graft copolymer were studied. Micellization and thermoresponsive behavior of PCL-*g*-PNIPAAm and its micelles were investigated. It is envisioned that the synthetic approach reported herein has several unique characters. First, the method reported in this study is efficient to prepare the thermoresponsive amphiphilic graft copolymers bearing the biodegradable polyester backbones and it represents the first report for the synthesis of such kind of graft copolymers. It can be generalizable to other graft copolymers bearing the polylactone backbone and vinyl polymer graft. Second, the grafting length and density can be tuned in this method, allowing for the feasible control of the structure and thermo-responsivity of assembled objects. Third, ARGET ATRP was used for the "grafting-from" polymerization instead of the conventional ATRP. Extremely small amount of copper catalyst was used in ARGET ATRP, which would be highly desired for the practical applications.

EXPERIMENTAL

Materials

ε-Caprolactone (CL; TCI, 99%) was dried over CaH_2 for 48 h and then distilled under reduced pressure. $CuCl_2$ (Acros Organics, 99%), dodecanol (Amethyst Chemicals, 99%), tin(II) 2-ethylhexanoate ($Sn(Oct)_2$; Aldrich-Sigma, 95%), and 3-chloroperbenzoic acid (mCPBA; Shanghai Dibo., 75%) were used as received. *N*-isopropylacrylamide (NIPAAm; J&K Chemical, 99%) was purified by recrystallization from *n*-hexane twice. Tris[2-(dimethylamino)-ethyl]amine (Me_6TREN) was synthesized according to a published method.[37,38] α-Chloro-ε-caprolactone (αClεCL) was synthesized by a reported method with small change (see Supporting Information).[23] Toluene, 1,4-dioxane, and isopropanol (Sinopharm Chemical Reagent) were first dried over CaH_2 and then distilled under reduced pressure. Other chemicals were used as received.

Synthesis of P(CL-*co*-αClεCL)

P(CL-*co*-αClεCL) random copolymers were synthesized *via* ROP by using dodecanol as the initiator and $Sn(Oct)_2$ as the catalyst. The synthetic procedure of P(CL-*co*-αClεCL) with an expected αClεCL mass fraction of 10% and molecular weight of 20 kg/mol is shown as below. αClεCL (2.0 g, 13.4 mmol), CL (18.0 g, 158 mmol), dodecanol (0.19 g, 1.0 mmol), and $Sn(Oct)_2$ (1.21 g, 3.0 mmol) were added into a flame-dried Schlenk flask. Then the flask was purged with dry argon and switch to vacuum again for more than three cycles. After injection of 30 mL of anhydrous toluene, the flask was immersed into an oil bath at 70°C and the polymerization was allowed to proceed at the same temperature for 48 h. After the reaction, the crude product was dissolved in chloroform and precipitated into ethanol thrice to remove the unreacted monomer. The product was finally dried *in vacuo* at 40°C for 24 h (yield: 15.6 g, 78%). The copolymers referred as P(CL-*co*-*x*αClεCL) with other compositions were prepared in a similar method, where *x* represented the feed ratio (in wt %) of αClεCL in monomers.

Synthesis of PCL-g-PNIPAAm

PCL-*g*-PNIPAAm graft copolymers were synthesized *via* ARGET ATRP by using Me_6TREN as the ligand and $Sn(Oct)_2$ as the *in situ* reducing agent. The synthesis of PCL10-*g*-PNIPAAm55 is described as below. P(CL-*co*−10%αClεCL) (0.38 g), NIPAAm (4.0 g, 35.4 mmol), $Sn(Oct)_2$ (0.72 g, 1.77 mmol), Me_6TREN (0.041 g, 0.18 mmol), and $CuCl_2$ (2.4 mg, 0.018 mmol) were introduced into a Schlenk flask. The flask was pulped and purged with dry argon. The mixed solvent of dioxane/isopropanol (16 mL, v/v, 1:1), which was degassed by bubbling with argon for 30 min, was injected into the flask. The polymerization was allowed to proceed at 60°C for 12 h under an argon

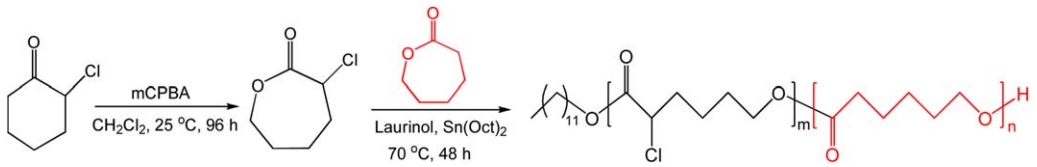

Scheme 1. Synthesis of P(CL-*co*-αClεCL) via ROP. [Color figure can be viewed in the online issue, which is available at wileyonlinelibrary.com.]

atmosphere. After the reaction, the reaction mixture was exposed to air and diluted with 80 mL of THF. It was then passed through a short alumina column to remove the catalyst complex. The crude copolymer was precipitated into cold ethyl ether from THF thrice to remove the unreacted monomer. The copolymer was then dried *in vacuo* at 40°C for 24 h. The graft copolymer is referred as PCL*x*-*g*-PNIPAAm*y*, where *x* is the expected weight ratio of αClεCL in P(CL-*co*-αClεCL) and *y* is the mean degree of polymerization of PNIPAAm grafts ($DP_{PNIPAAm}$).

Micelle Formation

The micelles of water-insoluble copolymers were prepared by a dialysis method. Briefly, the graft copolymer was dissolved in THF with a concentration of 3.0 g/L and then dialyzed against water (MWCO = 3500) for two days. The water was changed every six hours. For the water-soluble copolymers, they were directly dissolved into water (1.0 g/L) for micellation.

Characterization

^{1}H NMR spectra were measured on a 400 MHz Bruker AVANCE II NMR spectrometer (Bruker BioSpin, Switzerland) using $CDCl_3$ or D_2O as the solvent. NMR peaks of solvent were used as the references ($\delta = 7.26$ ppm for $CDCl_3$, $\delta = 4.79$ ppm for D_2O).

Fourier transform infrared (FTIR) spectra were recorded on a Nicolet 5700 spectrophotometer (ThermoElectron, Madison, USA) with 64 scans and a resolution of 2 cm^{-1}.

Molecular weights were measured on a gel permeation chromatography (GPC) consisted of a Waters degasser, a Waters 1515 isocratic HPLC pump, a Waters 2414 RI detector (Waters, Milford, MA, USA), and two PL-gel mix C columns at 60°C. DMF containing 0.05*M* LiBr was used as the eluent with a flow rate of 1.0 mL/min. Calibration was performed by the monodisperse poly(methyl methacrylate) (PMMA) standards.

Thermoresponsive behavior of copolymer micelles in the aqueous solution were measured by a UV-1800 UV-vis spectrophotometer (Shimazu, Kyoto, Japan) equipped with a temperature controller. The micelle solution with a concentration of 1.0 g/L was heated from 25°C to 50°C at a heating rate of 0.2°C/min. The absorbance (*A*) at a wavelength of 500 nm was recorded during the heating process. In order to see the cloud point more clearly, the absorbance was converted to transmittance in plotting ($T = 10^{-A} \times 100\%$).

Critical micelle concentration (CMC) was determined by the surface tension and dye solubilization methods. In the surface tension method,[19,39,40] the surface tensions of copolymer solutions with various concentrations (4×10^{-4}−1.0 g/L) were measured on a DataPhysics OCA 20 instrument (DataPhysics Instruments, Filderstadt, Germany). CMC was determined from the plot of surface tension versus copolymer concentration. For the dye solubilization method,[41,42] the hydrophobic dye, 1,6-diphenyl-1,3,5-hexatriene (DPH), was dissolved in methanol with a concentration of 0.6 m*M*. Then 30 μL of this solution was added into 3 mL of copolymer solution with various concentrations (2×10^{-4}−0.5 g/L) and equilibrated at 4°C for 48 h. UV-vis spectrum of this solution was measured on a UV-vis spectrophotometer (UV-1800, Shimazu, Kyoto, Japan). CMC was determined by the plot of the difference in absorbance at 378 and 400 nm *vs* logarithmic concentration.

Dynamic light scattering (DLS) analysis was conducted on a Zetasizer 3000 HSA instrument (Malvern Instruments, Malvern, UK) with a scattering angle of 90° at 23°C. The micelle solution with a concentration of 1.0 g/L was passed through a 0.45 μm pore-sized syringe filter before the measurement.

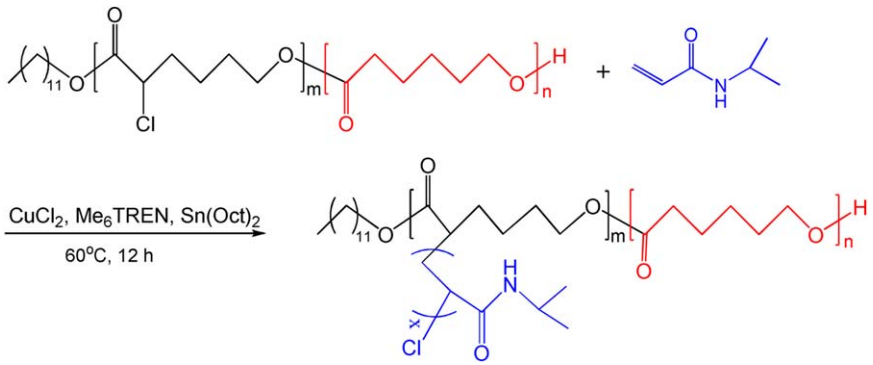

Scheme 2. Synthesis of PCL-*g*-PNIPAAm via ARGET ATRP. [Color figure can be viewed in the online issue, which is available at wileyonlinelibrary.com.]

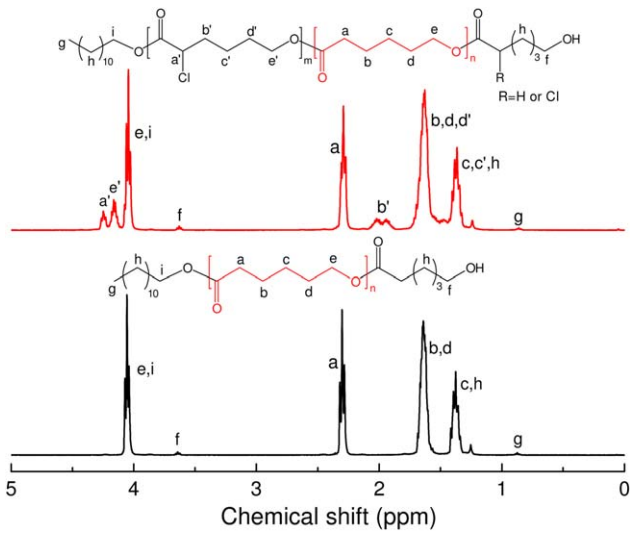

Figure 1. ^{1}H NMR spectra of PCL and P(CL-*co*−30%αClεCL). [Color figure can be viewed in the online issue, which is available at wileyonlinelibrary.com.]

Morphology of micelle particles was observed on a JEM-1230 transmission electron microscope (TEM, JEOL, Tokyo, Japan), operated at an acceleration voltage of 80 kV. The sample for TEM measurement was prepared by depositing one drop of micelle solution onto a carbon-coated copper grid. The sample was then dried *in vacuo* at room temperature for 48 h before the TEM imaging.

RESULTS AND DISCUSSION

Synthesis of P(CL-*co*-αClεCL)

Scheme 1 illustrates the synthesis of P(CL-*co*-αClεCL) and PCL-*g*-PNIPAAm graft copolymer. αClεCL was synthesized from α-chlorocyclohexanone and mCPBA *via* the Baeyer-Villiger oxidation.[23] P(CL-*co*-αClεCL) random copolymers were then prepared by the ROP of αClεCL and CL using $Sn(Oct)_2$ as the catalyst and dodecanol as the initiator. Content of chloro functionality in P(CL-*co*-αClεCL) was adjusted by the feed ratio of

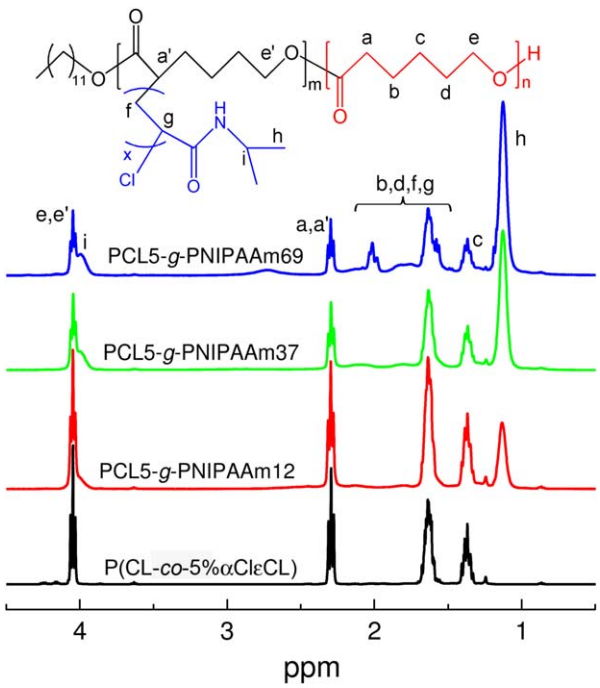

Figure 2. ^{1}H NMR spectra of P(CL-*co*-αClεCL) and PCL-*g*-PNIPAAm graft copolymers with different graft lengths. [Color figure can be viewed in the online issue, which is available at wileyonlinelibrary.com.]

αClεCL to CL. Figure 1 shows the ^{1}H NMR spectra of PCL homopolymer and P(CL-*co*-αClεCL) random copolymer. Except for the signals of PCL backbone, NMR spectrum of P(CL-*co*-αClεCL) exhibits triplets at 4.3 (peak a′) and 4.2 ppm (peak e′), assigning to the protons of methylidyne conjoint with chloro group (−C*H*Cl−) and the methylene conjoint with ester group (−CH_2COO−).

Feed ratio and molecular characteristics of P(CL-*co*-αClεCL) are shown in Table I. The molar ($n_{\alpha ClεCL}$) and mass fraction ($w_{\alpha ClεCL}$) of αClεCL unit in copolymer were calculated from the integral ratio of corresponding protons in the ^{1}H NMR spectra. As shown in Table I, $w_{\alpha ClεCL}$ is close to the weight fraction of

Table I. Feed Ratio, Composition, and Molecular Weight of PCL and P(CL-*co*-αClεCL)

	Feed ratio			Composition		Molecular weight			
Polymer	$\frac{\alpha ClεCL}{\alpha ClεCL+CL}$ (wt %)	$\frac{[M]_0}{[I]_0}$	Yield (%)	$n_{\alpha ClεCL}$[a] (mol%)	$w_{\alpha ClεCL}$[b] (wt %)	$M_{n,th}$[c] (kg/mol)	$M_{n,NMR}$[d] (kg/mol)	$M_{n,GPC}$ (kg/mol)	PDI
PCL	0	175.3	79	0	0	14.7	10.5	11.1	1.15
P(CL-*co*−5%αClεCL)	5	173.2	63	3.6	4.6	12.5	12.9	15.5	1.17
P(CL-*co*−10%αClεCL)	10	171.2	78	7.2	9.2	15.5	13.1	14.1	1.36
P(CL-*co*−20%αClεCL)	20	167.1	73	15.9	19.8	14.6	13.2	13.3	1.31
P(CL-*co*−30%αClεCL)	30	164.7	71	22.9	27.8	14.3	13.2	11.1	1.43

[a] $n_{\alpha ClεCL}=\frac{1/3\times(I_{a'ee'}-I_a)}{1/3\times(I_{a'ee'}-I_a)+1/2\times I_a}$, where I is the intensity of corresponding peak in NMR spectrum.

[b] $w_{\alpha ClεCL}=\frac{n_{\alpha ClεCL}\times 148.64}{n_{\alpha ClεCL}\times 148.64+(1-n_{\alpha ClεCL})\times 114.14}$.

[c] $M_{n,th}=\frac{[\alpha ClεCL]_0\times 148.64+[CL]_0\times 114.14}{[I]_0}\times$Yield, where $[\alpha ClεCL]_0$, $[CL]_0$, and $[I]_0$ are the initial molar concentrations of αClεCL, CL, and initiator in the reaction mixture.

[d] $M_{n,NMR}$ (PCL) $=\frac{1/4\times(I_a+I_a)\times 114.14}{1/3\times I_g}$, $M_{n,NMR}$ [P(CL-*co*-αClεCL)] $=\frac{1/2\times I_a\times 114.14+1/3\times(I_{a'ee'}-I_a)\times 148.64}{1/3I_g}$.

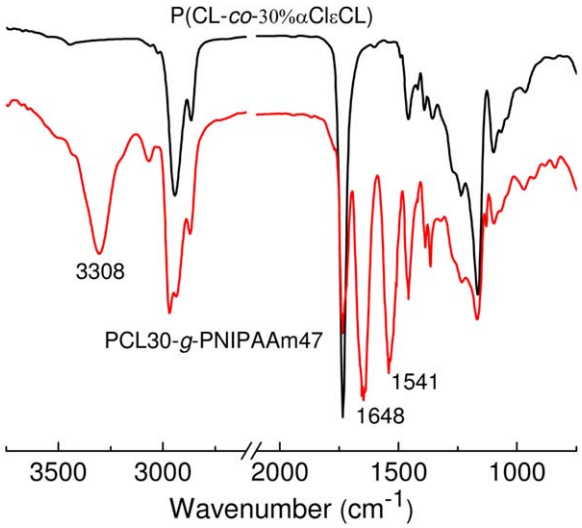

Figure 3. FTIR spectra of P(CL-*co*−30%αClεCL) and PCL30-*g*-PNIPAAm47 graft copolymer. [Color figure can be viewed in the online issue, which is available at wileyonlinelibrary.com.]

αClεCL in feeding. This indicates that the common catalyst, $Sn(Oct)_2$, is efficient for the ROP of CL and αClεCL and the copolymer composition can be well controlled by the feed ratio. The theoretical molecular weight ($M_{n,th}$) of P(CL-*co*-αClεCL) was calculated from the feed ratio and yield (Table I). The molecular weight, $M_{n,\ NMR}$, was also calculated by comparing the integral ratio of proton in PCL backbone and methyl proton of initiator end, based on the ^{1}H NMR spectra (Table I). As shown in Table I, the molecular weight measured by GPC ($M_{n,GPC}$) is close to $M_{n,th}$ and $M_{n,NMR}$, indicating the good control of ROP.

Synthesis of PCL-*g*-PNIPAAm

As compared to the conventional ATRP, ARGET ATRP allows the concentration of copper catalyst to be reduced to ppm level.[43] In ARGET ATRP, the activator is regenerated *in situ* from the deactivator complex, achieved by the employment of a

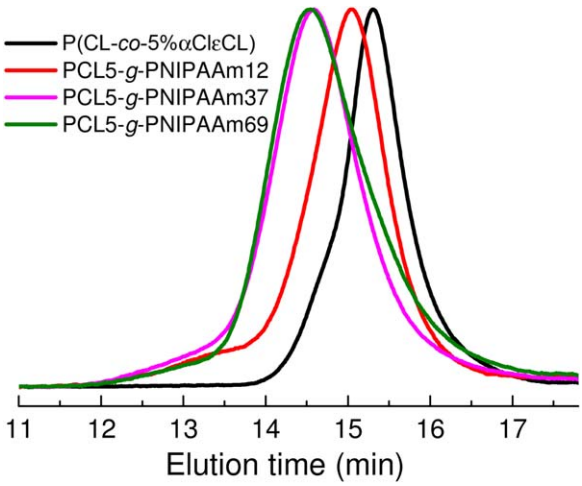

Figure 4. GPC traces of P(CL-*co*−5%αClεCL) and PCL5-*g*-PNIPAAm graft copolymers with different graft lengths. [Color figure can be viewed in the online issue, which is available at wileyonlinelibrary.com.]

Table II. Molecular Characteristics and Properties of PCL-*g*-PNIPAAm Graft Copolymers

Graft copolymer	Feed ratio $[NIPAAm]_0/[\alpha ClεCL]^a$	Composition		Molecular weight			Property			
		$DP_{PNIPAAm}{}^b$	w_{NIPAAm} (wt %)	$M_{n,NMR}{}^c$ (kg/mol)	$M_{n,GPC}$ (kg/mol)	PDI	Water solubility[d]	CMC (mg/L)[e]	D_h (nm)	LCST (°C)
PCL5-*g*-PNIPAAm12	50	12	27.2	21.4	17.6	1.24	−	6.4	26.0	34.6
PCL5-*g*-PNIPAAm37	100	37	55.8	35.5	24.1	1.40	−	8.2	99.6	34.7
PCL5-*g*-PNIPAAm69	150	69	70.6	53.4	25.6	1.40	+	17.4	117.3	31.6
PCL10-*g*-PNIPAAm20	50	20	57.6	33.8	27.6	1.32	−	8.6	47.3	32.2
PCL10-*g*-PNIPAAm55	150	55	78.8	68.3	33.5	1.53	+	19.5	111.7	31.8
PCL20-*g*-PNIPAAm53	100	53	88.0	117.2	48.8	1.75	+	21.3	104.3	31.6
PCL30-*g*-PNIPAAm47	100	47	90.1	121.3	62.6	1.80	+	23.4	94.9	31.0

[a] Molar feed ratio of NIPAAm to αClεCL unit.
[b] $DP_{PNIPAAm} = \frac{1/2\times(I_{e,e'}-1/6\times I_h)\times n_{\alpha ClεCL}}{1/6\times I_h}$.
[c] $M_{n,NMR} = \left[1+\frac{n_{\alpha ClεCL}\times DP_{NIPAAm}\times 113.16}{n_{\alpha ClεCL}\times 14864+(1-n_{\alpha ClεCL})\times 114.14}\right]\times M_{n,GPC}$ (PCL), where $M_{n,GPC}$(PCL) is M_n of PCL backbone measured by GPC.
[d] Water solubility of copolymer (1.0 g/L) in water at 25°C. +, soluble; −, insoluble.
[e] CMC was derived from the surface tension method.

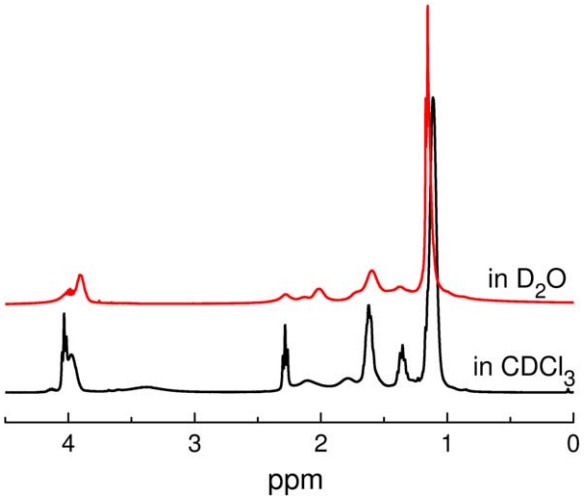

Figure 5. ^{1}H NMR spectra of PCL30-*g*-PNIPAAm47 graft copolymer in $CDCl_3$ and D_2O. [Color figure can be viewed in the online issue, which is available at wileyonlinelibrary.com.]

reducing agent. PCL-*g*-PNIPAAm graft copolymers were prepared via a "grafting-from" ARGET ATRP method using P(CL-*co*-αClεCL) as a macroinitiator, copper (II) as a catalyst, and $Sn(Oct)_2$ as a reducing agent. The molar feed ratio of $[NIPAAm]/[Sn(Oct)_2]/[Me_6TREN]/[CuCl_2]$ was kept to be 200/10/1/0.1. The chemical structure of graft copolymers was characterized by NMR, FTIR, and GPC. As shown in Figure 2, ^{1}H NMR spectra of copolymers show the resonance peaks at 3.9–4.0 and 1.1–1.2 ppm, characteristic of the methine and methyl protons of PNIPAAm isopropyl groups, respectively. With the length of graft chain growing, the NMR peak intensities of PNIPAAm segment (e.g., peaks i and h) increase and those of PCL backbone (peaks a, e) decrease. Meanwhile, the methine proton signal of $-CH\text{Cl}-$ in PCL (4.3 ppm) disappears after the graft polymerization. In the FTIR spectra (Figure 3), the characteristic absorptions of PNIPAAm at 3308 cm^{-1} (N-H stretching), 1648 cm^{-1} (C=O stretching), 1541 cm^{-1} (N-H bending)[44] are observed. In the GPC curves (Figure 4), the graft copolymers exhibit sharp elution peaks with the relatively narrow molecular weight distributions. GPC peak shifts to shorter retention time as the NIPAAm/P(CL-*co*-αClεCL) feed ratio or graft length increases. All the NMR, FTIR, and GPC results confirm the successful synthesis of PCL-*g*-PNIPAAm.

Molecular characteristics of PCL-*g*-PNIPAAm are listed in Table II. The mean degree of polymerization of PNIPAAm graft chains ($DP_{PNIPAAm}$) and mass fraction of PNIPAAm in the copolymer (w_{NIPAAm}) were calculated from the ^{1}H NMR spectra. As seen in Table II, $DP_{PNIPAAm}$, which is proportional to the graft length, increases as the NIPAAm/P(CL-*co*-αClεCL) feed ratio increases. For the "grafting-from" method, the graft density can be changed by varying the concentration of active initiation sites in the macroinitiator. Therefore, the length and density of grafting chains can be tuned in this "grafting-from" ARGET ATRP method, allowing the feasible control of copolymer composition.

Molecular weights of graft copolymers were measured by GPC and also estimated from the ^{1}H NMR spectra. As seen in Table II, $M_{n,GPC}$ is smaller than $M_{n,NMR}$, which is more dominant for the copolymers having longer or denser grafting chains. This is because of the fact that the molecular weight of graft polymer is underestimated in the GPC analysis when the linear polymers are used as standards. It is notable that the solubility of graft copolymer strongly depends on the copolymer composition. The copolymers containing less PNIPAAm segments ($w_{NIPAAm} < 70\%$) are insoluble, while those with more hydrophilic PNIPAAm segments ($w_{NIPAAm} > 70\%$) are soluble in water at 25°C (Table II).

Micellization of PCL-*g*-PNIPAAm

Because the PCL-*g*-PNIPAAm copolymers are amphiphilic at room temperature, it is expected that they can self-assemble into micelles in the aqueous solution. NMR spectroscopy was used to investigate the effect of solvent on the self-assembled structure.[10,12,13,45] Figure 5 shows the NMR spectra of a water-soluble graft copolymer (i.e., PCL30-*g*-PNIPAAm47) in $CDCl_3$ and D_2O. $CDCl_3$ is a good solvent for both PCL and PNIPAAm. D_2O is a selective solvent for PNIPAAm but poor for PCL. As shown in Figure 5, in $CDCl_3$, all the characteristic signals of

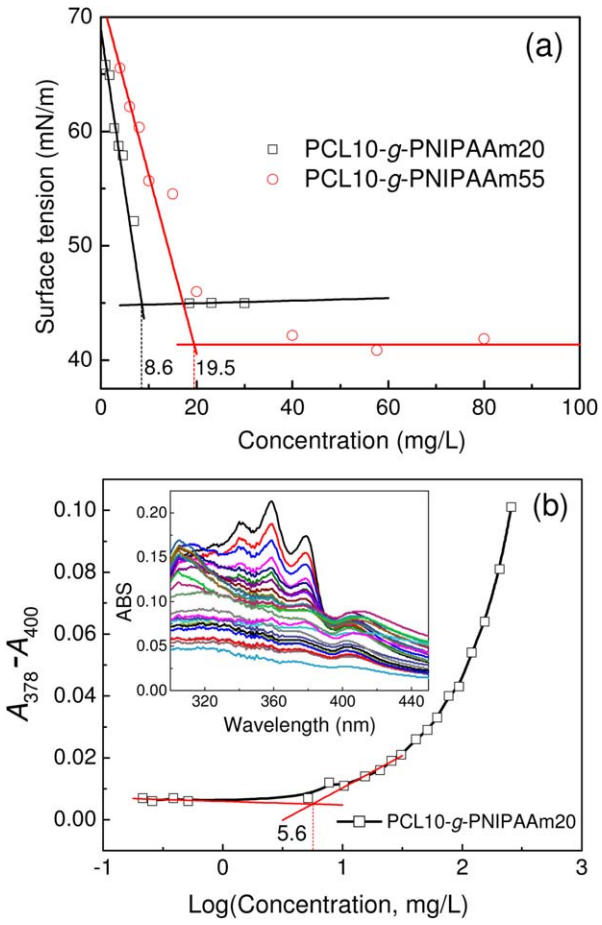

Figure 6. CMC determination by the extrapolation of (a) surface tension and (b) difference in absorbance at 378 and 400 nm for the copolymer solutions with different concentrations. Inset of part b shows the change of UV-vis spectra for DPH with increasing the concentration of PCL10-*g*-PNIPAAm20. [Color figure can be viewed in the online issue, which is available at wileyonlinelibrary.com.]

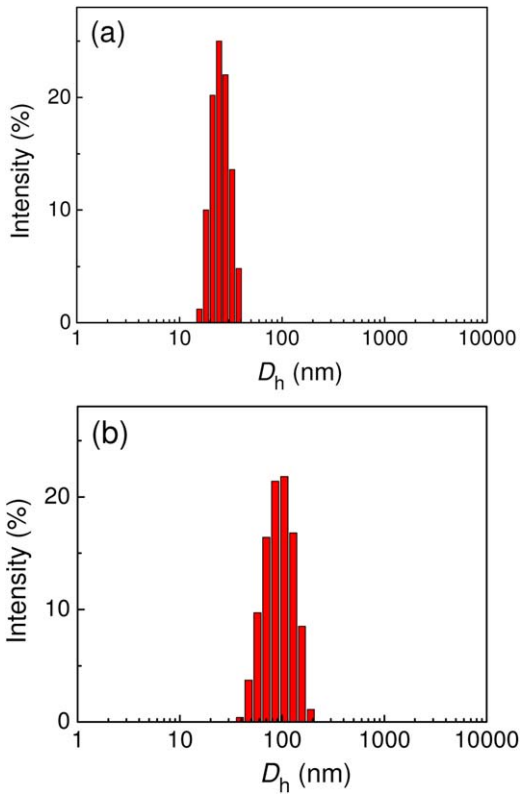

Figure 7. Particle size distribution of (a) PCL5-*g*-PNIPAAm12 and (b) PCL5-*g*-PNIPAAm37 micelles in water. [Color figure can be viewed in the online issue, which is available at wileyonlinelibrary.com.]

PNIPAAm and PCL are sharp and clearly visible, indicating that both blocks are molecularly solvated. However, in D_2O, only the peaks of PNIPAAm are sharp and well-defined while those of PCL are broad. This suggests that the graft copolymers self-assemble into the core-shell micelle comprised of the hydrophobic PCL core surrounded by the hydrophilic PNIPAAm corona in the aqueous solution.[10,12,13]

The CMC of graft copolymer was measured by the surface tension and dye solubilization methods. When the concentration of amphiphilic copolymer is approaching CMC, its surface tension undergoes an abrupt change. As shown in Figure 6(a), CMC was estimated from the inflection of the surface tension versus concentration plot.[19,39,40] Below CMC, the surface tension changes strongly with copolymer concentration. While above CMC, the surface tension remains relatively constant. For the dye solubilization method, the hydrophobic dye will transfer from the aqueous phase into micelle core when the copolymer concentration is increased to above CMC, leading to the drastic increase of absorption coefficient of dye. As shown in Figure 6(b), CMC corresponds to the concentration with the sudden increase of absorbance. As exemplified by PCL10-*g*-

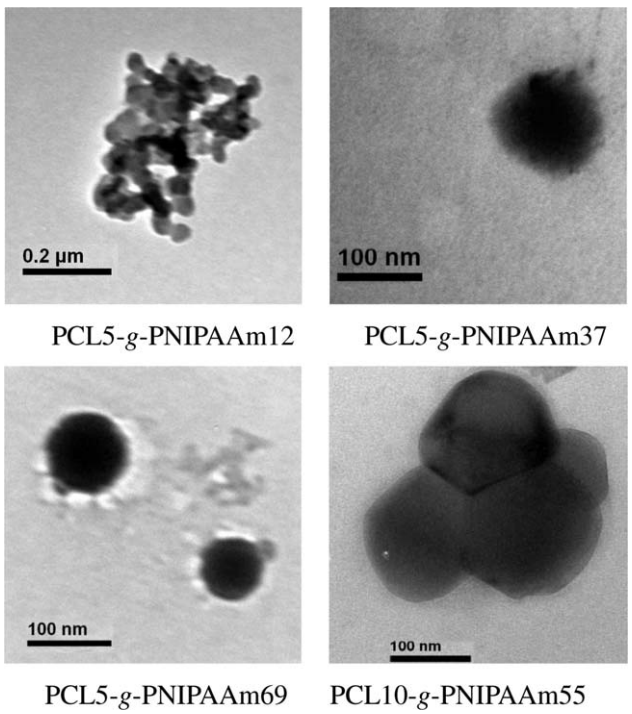

Figure 8. TEM micrographs of PCL-*g*-PNIPAAm micelles.

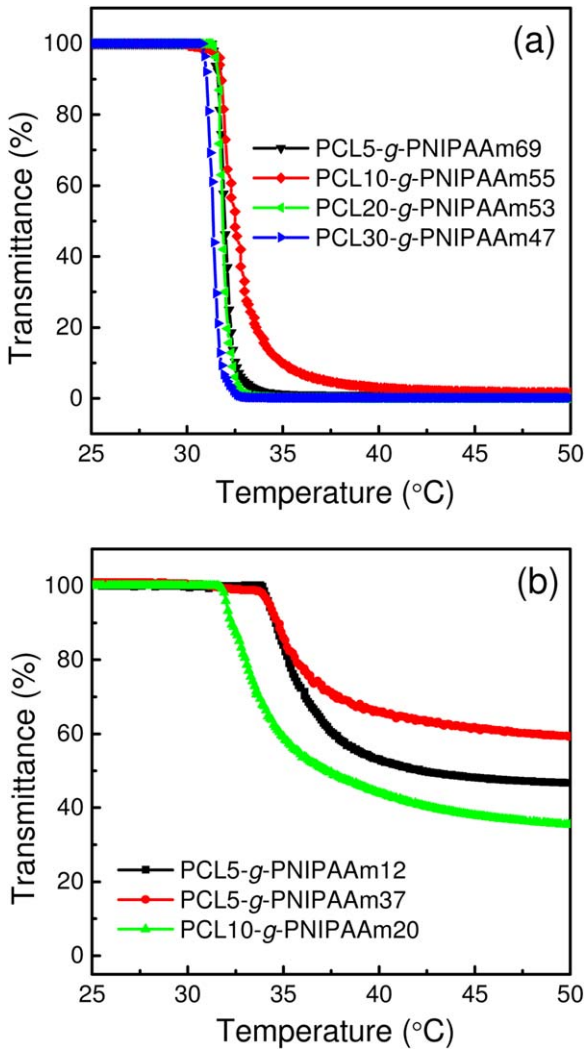

Figure 9. Temperature-dependent transmittance (at 500 nm) for the micelle solutions of PCL-*g*-PNIPAAm graft copolymers (1.0 g/L) upon heating at a rate of 0.2°C/min. [Color figure can be viewed in the online issue, which is available at wileyonlinelibrary.com.]

PNIPAAm20, its CMC measured by dye solubilization method (5.6 mg/L) is similar to that derived from the surface tension method (8.6 mg/L), considering the measurement error of CMC.

As shown in Table II, CMC of graft copolymer depends strongly on the composition. This composition-dependent CMC has also been reported for the PNIPAAm-*b*-PCL-*b*-PNIPAAm[12] and PCL-*b*-PNIPAAm-*b*-PCL[13] triblock copolymers. It increases from 6.4 to 23.4 mg/L as the mass fraction of PNIPAAm increases from 27.2% to 90.1%. CMC of the water-insoluble copolymer is less than 10 mg/L, while that of the water-soluble one is several tens of mg/L. CMC of PCL-*g*-PNIPAAm increases with the increase in graft length and density of PNIPAAm. For the graft copolymers with P(CL-*co*−5%αClεCL) as backbone, CMC increases from 6.4 to 17.4 mg/L as the $DP_{PNIPAAm}$ increases from 12 to 69. CMC of PCL-*g*-PNIPAAm is similar to that of the PNIPAAm-*b*-PCL-*b*-PNIPAAm copolymers reported by Li and coworker.[12] They have reported that the triblock copolymers containing 66–86 wt % PNIPAAm segment have the CMC values of 6.9–18.2 mg/L.[12]

The size and morphology of copolymer micelles were identified by DLS and TEM. As shown in Figure 7, the hydrodynamic diameter (D_h) of micelle exhibits a single peak in the distribution curve. D_h is strongly dependent on the copolymer composition. It ranges from 26.0 to 117.3 nm with the graft length and density varying (Table II). D_h values of graft copolymers containing 70–90 wt % PNIPAAm segment are in the range of 94.9–117.3 nm, which are similar as those of the PNIPAAm-*b*-PCL-*b*-PNIPAAm copolymers (PNIPAAm content = 66–86 wt %, D_h = 92–125 cm)[12] while slightly smaller than those of the PCL-*b*-PNIPAAm-*b*-PCL copolymers (D_h =141–196 cm).[13]

As shown in Figure 8, the micelles of graft copolymers have spherical morphology. PCL5-*g*-PNIPAAm12 forms the smaller micelles than PCL5-*g*-PNIPAAm37, PCL5-*g*-PNIPAAm69, and PCL10-*g*-PNIPAAm55, consistent with the DLS results. The graft copolymers with longer PNIPAAm segments form larger micelles, because of the increased length of micelle coronas. For the PCL-*g*-PNIPAAm copolymers with P(CL-*co*−5%αClεCL) as backbone, D_h increases from 26.0 to 117.3 nm as $DP_{PNIPAAm}$ increases from 12 to 69. Moreover, D_h slightly increases as the mass fraction or graft density of PNIPAAm decreases, because the micelle particles with larger cores will be formed to include all the insoluble chains for the copolymers containing more core-forming segments.[46]

Thermoresponsive Behavior of PCL-*g*-PNIPAAm Micelles

Thermoresponsive behavior of PCL-*g*-PNIPAAm micelles was investigated by the UV-vis spectrometer (Figure 9). Because of the dehydration of PNIPAAm at higher temperature, the stretched PNIPAAm chains located in the micelle corona will collapse from an extended-coil to shrunken-globule conformation; this will destabilize the micelle colloid and leads to the inter-micelle aggregation. Therefore, the micelle solutions of PCL-*g*-PNIPAAm copolymers show abrupt decrease in transparency upon heating, as shown in Figure 9. The cloud point was evaluated from the temperature with 90% transmittance. As shown in Table II, the water-soluble PCL-*g*-PNIPAAm has a cloud point ranging 31–32°C, similar as the PNIPAAm-*b*-PCL-*b*-PNIPAAm triblock copolymer with the comparable PNIPAAm and PCL mass ratios.[12] Because the clouding of PCL-*g*-PNIPAAm micelles in heating is caused by the hydrophilic-to-hydrophobic transition of PNIPAAm segments, the micelles with the shorter PNIPAAm in corona layer will have a higher cloud point. Therefore, the micelle of water-insoluble copolymer exhibits a higher cloud point [Table II, Figure 9(b)], albeit the higher content of PCL segment.

CONCLUSIONS

Thermoresponsive and amphiphilic PCL-*g*-PNIPAAm graft copolymers with well-defined structure were successfully synthesized by a new route combining the ROP of lactone monomers and "grafting from" ARGET ATRP of the another monomer. The graft length and density were well controlled by the feed ratio and the fraction of chlorides along the PCL backbone, which acted as the macroinitiator. Moreover, the developed molecular weight and composition of PCL-*g*-PNIPAAm were consistent with the designed molecular characters. PCL-*g*-PNIPAAm can self-assemble into spherical core-shell micelles in aqueous solution and the CMC of copolymer increases as the PNIPAAm content increases. The size of PCL-*g*-PNIPAAm micelles can be tuned in a wide range of 26.0–117.3 nm and it increases with the growing length of PNIPAAm segment. The PCL-*g*-PNIPAAm micelles are thermoresponsive and aggregate above LCST. This class of thermoresponsive graft copolymers containing the biodegradable and biocompatible backbone may find potential applications for the carrying and releasing of hydrophobic drugs.

ACKNOWLEDGMENTS

This work was financially supported by the Natural Science Foundation of China (51103127 and 21274128), State Key Laboratory of Chemical Engineering (SKL-ChE-11D05 and SKL-ChE-12D06), and Fundamental Research Funds for the Central Universities (2013FZA4019).

REFERENCES

1. Riess, G. *Prog. Polym. Sci.* **2003**, *28*, 1107.
2. Blanazs, A.; Armes, S. P.; Ryan, A. *J. Macromol. Rapid Commun.* **2009**, *30*, 267.
3. Tian, H. Y.; Tang, Z. H.; Zhuang, X. L.; Chen, X. S.; Jing, X. B. *Prog. Polym. Sci.* **2012**, *37*, 237.
4. Wei, H.; Cheng, S. X.; Zhang, X. Z.; Zhuo, R. X. *Prog. Polym. Sci.* **2009**, *34*, 893.
5. Hoffman, A. S.; Stayton, P. S. *Prog. Polym. Sci.* **2007**, *32*, 922.
6. Kohori, F.; Sakai, K.; Aoyagi, T.; Yokoyama, M.; Sakurai, Y.; Okano, T. *J. Control. Release* **1998**, *55*, 87.
7. Liu, S. Q.; Yang, Y. Y.; Liu, X. M.; Tong, Y. W. *Biomacromolecules* **2003**, *4*, 1784.
8. You, Y. Z.; Hong, C. Y.; Wang, W. P.; Lu, W. Q.; Pan, C. Y. *Macromolecules* **2004**, *37*, 9761.
9. Hales, M.; Barner-Kowollik, C.; Davis, T. P.; Stenzel, M. H. *Langmuir* **2004**, *20*, 10809.
10. Choi, C.; Chae, S. Y.; Nah, J. W. *Polymer* **2006**, *47*, 4571.
11. Choi, C.; Jang, M. K.; Nah, J. W. *Macromol. Res.* **2007**, *15*, 623.

12. Loh, X. J.; Wu, Y. L.; Seow, W. T. J.; Norimzan, M. N. I.; Zhang, Z. X.; Xu, F. J.; Kang, E. T.; Neoh, K. G.; Li, J. *Polymer* **2008**, *49*, 5084.
13. Chang, C.; Wei, H.; Quan, C. Y.; Li, Y. Y.; Liu, J.; Wang, Z. C.; Cheng, S. X.; Zhang, X. Z.; Zhuo, R. X. *J. Polym. Sci. Part A: Polym. Chem.* **2008**, *46*, 3048.
14. Quan, C. Y.; Wu, D. Q.; Chang, C.; Zhang, G. B.; Cheng, S. X.; Zhang, X. Z.; Zhuo, R. X. *J. Phys. Chem. C* **2009**, *113*, 11262.
15. Sun, P. J.; Zhang, Y.; Shi, L. Q.; Gan, Z. H. *Macromol. Biosci.* **2010**, *10*, 621.
16. Chen, W. Q.; Wei, H.; Li, S. L.; Feng, J.; Nie, J.; Zhang, X. Z.; Zhuo, R. X. *Polymer* **2008**, *49*, 3965.
17. Wei, H.; Chen, W. Q.; Chang, C.; Cheng, C.; Cheng, S. X.; Zhang, X. Z.; Zhuo, R. X. *J. Phys. Chem. C* **2008**, *112*, 2888.
18. Yang, Z.; Xie, J. D.; Zhou, W.; Shi, W. F. *J. Biomed. Mater. Res. A* **2009**, *89A*, 988.
19. Li, Y. Y.; Zhang, X. Z.; Cheng, H.; Zhu, J. L.; Cheng, S. X.; Zhuo, R. X. *Macromol. Rapid Commun.* **2006**, *27*, 1913.
20. Zhu, J. L.; Zhang, X. Z.; Cheng, H.; Li, Y. Y.; Cheng, S. X.; Zhuo, R. X. *J. Polym. Sci. Part A: Polym. Chem.* **2007**, *45*, 5354.
21. Parrish, B.; Breitenkamp, R. B.; Emrick, T. *J. Am. Chem. Soc.* **2005**, *127*, 7404.
22. Detrembleur, Ch.; Mazza, M.; Halleux, O.; Lecomte, Ph.; Mecerreyes, D.; Hedrick, J. L.; Jérôme, R. *Macromolecules* **2000**, *33*, 14.
23. Lenoir, S.; Riva, R.; Lou, X.; Detrembleur, Ch.; Jérôme, R.; Lecomte, Ph. *Macromolecules* **2004**, *37*, 4055.
24. Wang, G. J.; Shi, Y.; Fu, Z. F.; Yang, W. T.; Huang, Q. G.; Zhang, Y. D. *Polymer* **2005**, *46*, 10601.
25. El Habnouni, S.; Blanquer, S.; Darcos, V.; Coudane, J. *J. Polym. Sci. Part A: Polym. Chem.* **2009**, *47*, 6104.
26. Al-Azemi, T. F.; Mohamod, A. A. *Polymer* **2011**, *52*, 5431.
27. Xu, N.; Wang, R.; Du, F. S.; Li, Z. C. *J. Polym. Sci. Part A: Polym. Chem.* **2009**, *47*, 3583.
28. Nottelet, B.; Darcos, V.; Coudane, J. *J. Polym. Sci. Part A: Polym. Chem.* **2009**, *47*, 5006.
29. Massoumi, B.; Abdollahi, M.; Fathi, M.; Entezami, A. A.; Hamidi, S. *J. Polym. Res.* **2013**, *20*, 47.
30. Riva, R.; Rieger, J.; Jérôme, R.; Lecomte, Ph. *J. Polym. Sci. Part A: Polym. Chem.* **2006**, *44*, 6015.
31. Riva, R.; Schmeits, S.; Jérôme, C.; Jérôme, R.; Lecomte, Ph. *Macromolecules* **2007**, *40*, 796
32. Li, H. Y.; Riva, R.; Jérôme, R.; Lecomte, Ph. *Macromolecules* **2007**, *40*, 824.
33. Lee, R. S.; Huang, Y. T. *J. Polym. Sci. Part A: Polym. Chem.* **2008**, *46*, 4320.
34. Darcos, V.; Al Tabchi, H.; Coudane, J. *Eur. Polym. J.* **2011**, *47*, 187.
35. Zhang, K.; Wang, Y.; Zhu, W. P.; Li, X. D.; Shen, Z. Q. *J. Polym. Sci. Part A: Polym. Chem.* **2012**, *50*, 2045.
36. Yao, K. J.; Tang, C. B.; Zhang, J.; Bunyard, C. *Polym. Chem.* **2013**, *4*, 528.
37. Britovsek, G. J. P.; England, J.; White, A. J. P. *Inorg. Chem.* **2005**, *44*, 8125.
38. Xia, J. H.; Gaynor, S. G.; Matyjaszewski, K. *Macromolecules* **1998**, *31*, 5958.
39. Kickelbick, G.; Bauer, J.; Huesing, N.; Andersson, M.; Holmberg, K. *Langmuir* **2003**, *19*, 10073.
40. Cao, Z. Q.; Liu, W. G.; Ye, G. X.; Zhao, X. L.; Lin, X. Z.; Gao, P.; Yao, K. D. *Macromol. Chem. Phys.* **2006**, *207*, 2329.
41. Alexandridis, P.; Holzwarth, J. F.; Hatton, T. A. *Macromolecules* **1994**, *27*, 2414.
42. Loh, X. J.; Goh, S. H.; Li, J. *Biomacromolecules* **2007**, *8*, 585.
43. Jakubowski, W.; Matyjaszewski, K. *Macromolecules* **2005**, *38*, 4139.
44. Pan, P. J.; Fujita, M.; Ooi, W.-Y.; Sudesh, K.; Takarada, T.; Goto, A.; Maeda, M. *Polymer* **2011**, *52*, 895.
45. Guo, S. T.; Wang, W. W.; Deng, L. D.; Xing, J. F.; Dong, A. *J. Macromol. Chem. Phys.* **2010**, *211*, 1572.
46. Pan, P. J., Fujita, M.; Ooi, W.-Y.; Sudesh, K.; Takarada, T.; Goto, A.; Maeda, M. *Langmuir* **2012**, *28*, 14347.